A Simulation of Atmospheric Blocking with a Forced Barotropic Model

JEFFREY L. ANDERSON

Geophysical Fluid Dynamics Laboratory, Princeton, New Jersey

(Manuscript received 16 March 1994, in final form 12 October 1994)

ABSTRACT

Nearly stationary states (NSSs) of the barotropic vorticity equation (BVE) on the sphere that are closely related to observed atmospheric blocking patterns have recently been derived. Examining the way such NSSs affect integrations of the BVE is of interest. Unfortunately, the BVE rapidly evolves away from the neighborhood of blocking NSSs due to instability and never again generates sufficient amplitude to return to the vicinity of the blocking NSSs. However, forced versions of the BVE with both a high amplitude blocking NSS and more zonal low amplitude NSSs can be constructed. For certain parameter ranges, extended integrations of these forced BVEs exhibit two "regimes," one strongly blocked and the other relatively zonal. Somewhat realistic simulations of low and high frequency variability and individual blocking event life cycles are also produced by these forced barotropic models. It is argued here that these regimes are related to "attractor-like" behavior of the NSSs of the forced BVE. Strong barotropic short waves apparently provide the push needed to cause a transition to or from the blocked regime. In the purely barotropic model used here, there is a rather delicate balance required between the forcing strength for different spatial scales in order to produce regimelike behavior. However, the mechanism proposed appears to be a viable candidate for explaining the observed behavior of blocking events in the atmosphere.

1. Introduction

Atmospheric blocks can have a profound effect upon surface weather conditions because of their high amplitude, low-frequency nature. It has long been suspected that blocking events may be more readily predicted than other midlatitude weather features because they are inherently low-frequency events. Because blocks have long lifetimes compared to many other midlatitude phenomena, one possible approach to understanding blocks has been to study solutions of appropriate model equations that have zero, or very small, time tendencies. If such nearly stationary solutions exist, and if they resemble observed blocking events in some way, it is natural to offer such solutions as partial explanation of the existence of blocks.

Because of their simplicity, barotropic models have received the greatest amount of attention in the search for stationary states. In this study, attention is confined to variants of the barotropic vorticity equation (BVE) on a sphere. A number of classes of stationary solutions of the BVE on the sphere are known, ranging from zonal flows through Rossby–Haurwitz waves (Hoskins 1973) to the relatively newly discovered modon solutions. Modons are stationary (or uniformly propagating) solutions that have at least one localized region in which the relationship between streamfunction and absolute vorticity has a different structure than in surrounding regions (Tribbia 1984; Neven 1992). A number of classes of modon solutions on the sphere can be constructed analytically, and many of these have a localized dipole structure that is reminiscent of the high over low behavior often noted in observed atmospheric blocking events (Verkley 1987). This similarity between modon solutions and atmospheric blocks is suggestive, but does not provide conclusive evidence that modon-like solutions of the full governing equations of the atmosphere are influencing the evolution of the atmospheric flow.

Solutions of the BVE that are nearly stationary and are also "close" to observed atmospheric blocking states can be constructed using numerical techniques. Pioneering work on this approach was performed by Branstator and Opsteegh (1989, hereafter BrO). More recently, Anderson (1992) was able to produce nearly stationary states (NSSs) by using an algorithm to minimize globally integrated BVE time tendency starting with an observed atmospheric flow pattern. The resulting NSSs displayed distinctive dipole patterns that are locally quite similar to those found in analytically derived modon solutions. Again, this suggests a possible link between dipole NSSs of the BVE and observed blocking events, but provides very little information about the dynamics that might be responsible for such a link.

A number of studies have attempted to clarify the relation between the existence of multiple stationary

Corresponding author address: Dr. Jeffrey L. Anderson, Geophysical Fluid Dynamics Laboratory, Princeton University, P.O. Box 308, Princeton, NJ 08542.

solutions of the BVE and the existence of regime-like behavior. Pierrehumbert and Malguzzi (1984, hereafter PM) demonstrated the existence of multiple equilibria in a forced beta-plane version of the BVE. They produced a model with one low-amplitude equilibrium, which they identified with zonal flow, and a second high-amplitude "blocking" equilibrium. Beginning with Charney and DeVore (1979), a series of papers examined the dynamics of highly truncated models of flow over topography that demonstrated multiple equilibria. Benzi et al. (1984, 1988) extended Charney and DeVore's results, examining in particular the roles of wave–wave interaction in transitions between equilibria. Branstator and Opsteegh studied a similar forcing in the BVE on the sphere and found evidence of two "attractors" influencing the evolution of the model. These studies provide a great deal of the foundation for this work.

A different approach to explaining blocking can be found in Shutts (1983). Blocking is viewed as a by-product of the interaction of high-frequency synoptic-scale waves and a low-frequency planetary wave field. A region of diffluent flow in the planetary wave field is viewed as providing the potential for blocking. Energy from incoming short waves can, under the appropriate circumstances, interact with the background long-wave field and result in the formation of a high amplitude blocking event. Similarly, shortwave propagation is also viewed as the mechanism for destruction of blocking events. Blocks are either destroyed by the arrival of a strong short wave from upstream (Shutts 1986) or gradually lose energy through downstream propagation of energy.

This view of blocking as an interaction between a nearly stationary diffluent low-frequency planetary wave field and large amplitude synoptic-scale transient waves is used as a guide in approaching the forced multiple equilibria theory of PM and BrO. The BVE will be forced toward a nearly stationary state of the unforced BVE as in BO. However, the forcing is chosen to be scale selective so that planetary-scale waves are very strongly forced, while "synoptic scale" waves are only very weakly forced. The long waves are thus constrained to provide a diffluent region for the formation of blocks, while short waves will propagate freely in order to provide energy for possible block formation or destruction.

Section 2 provides a description of the forced barotropic vorticity equation and the NSS that is used for forcings in the experiments described here. Section 3 presents the results of some long integrations of this forced BVE in terms of a "blocking" index. Section 4 provides further discussion of the relation between NSSs of the forced equation and blocking behavior. Section 5 examines the sensitivity of the forced BVE to changes in a variety of parameters, while sections 6 and 7 present discussion and conclusions.

2. Experimental design

a. Barotropic vorticity equation

This paper studies the behavior of several variants of the barotropic vorticity equation (BVE) on the sphere

$$\partial\nabla^2\psi/\partial t = -J(\psi, q). \tag{1}$$

In (1), ψ is the streamfunction, $q = \nabla^2\psi + f$ is the absolute vorticity, f the Coriolis parameter, ∇^2 the horizontal Laplacian on the sphere, and $J(\ ,\ )$ the spherical Jacobian operator.

Throughout the following, a truncated set of spherical harmonics is used to represent quantities on the sphere. For instance, the relative vorticity field can be represented as

$$\nabla^2\psi = \zeta = \mathrm{Re}\{\sum_{m=-N}^{N}\sum_{n=|m|}^{N}\zeta_n^m P_n^m(\sin\theta)e^{im\lambda}\}. \tag{2}$$

In (2), P_n^m is an associated Legendre function of order m and degree n, θ is latitude, λ longitude, m the meridional wavenumber, and n is the total wavenumber. The truncation represented in (2) is triangular, and, unless otherwise noted, T21 truncation ($N = 21$) is used.

b. Free nearly stationary states

A variety of nearly stationary solutions (NSSs) of the unforced BVE (1) have recently been derived by BrO and Anderson (1992). A single-valued metric of the total time tendency for a given streamfunction in (1) is minimized to produce these NSSs, with initial conditions for the minimization chosen from observed streamfunction patterns. The construction of the NSS is performed by successive modification of the observed streamfunction field.

For the NSSs used here, the functional to be minimized is the same as in Anderson,

$$F = \sum_i [J(\psi, q)]_i^2, \tag{3}$$

where the sum is over the real and imaginary parts of all coefficients in the spectral representation of the Jacobian. A relatively standard conjugate gradient algorithm, if applied with care, can be used to minimize F. In general, such algorithms require a computation of the gradient of F with respect to ψ. The gradient for F in equations such as (1) can be computed using the corresponding adjoint linear tangent equation.

The results presented here concentrate on a single NSS of (1) corresponding to the 14 January 1987,300-mb European Centre for Medium-Range Weather Forecasting streamfunction analysis. This analysis contains a significant block over Europe, which results in a strong dipole pattern in the corresponding NSS.

Figure 1 displays the Northern Hemisphere NSS streamfunction pattern for 14 January 1987, while Fig.

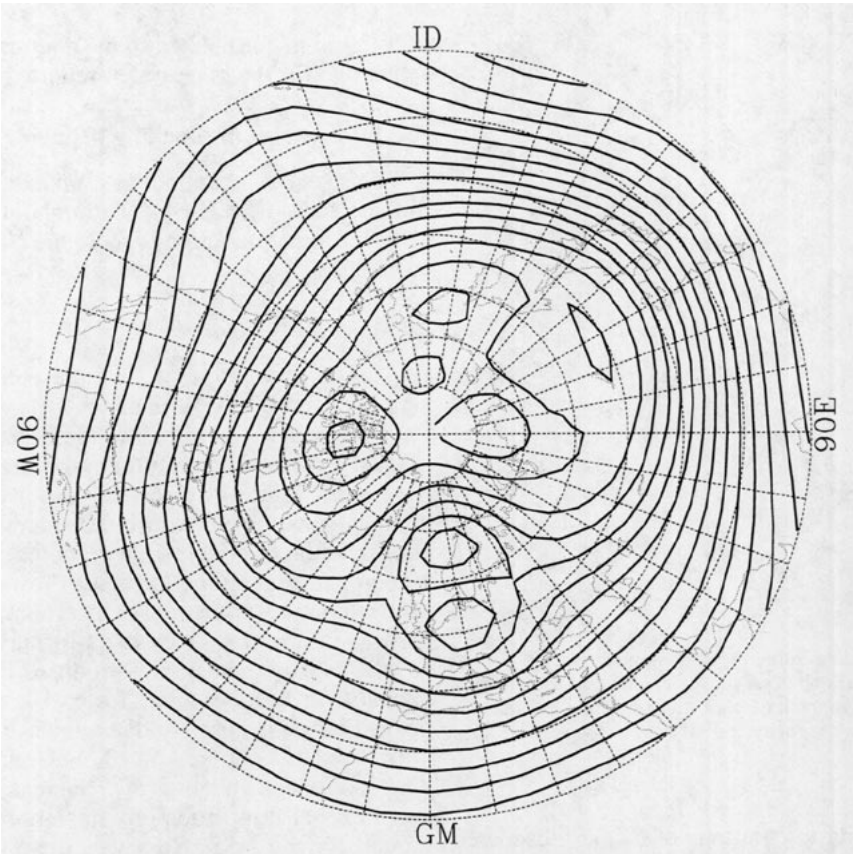

FIG. 1. Northern Hemisphere streamfunction for nearly stationary state corresponding to 14 January 1987 300 mb, contour interval 1×10^7 m^2 s^{-1}.

2 displays the corresponding $q-\psi$ plot. In the construction of this NSS, the conjugate gradient minimization was terminated after 1000 iterations, when F had been reduced by nearly six orders of magnitude.

The $q-\psi$ plot (Read et al. 1986; Butchart et al. 1989) displays the values of absolute vorticity q versus streamfunction ψ for each physical space point on the Gaussian grid corresponding to the spectral representation (2). One distinctive feature of Fig. 2 is the nearly linear set of points corresponding to the "blocking" dipole region over Europe in the NSS streamfunction. This line demonstrates that there is a distinct quasi-linear relation between q and ψ inside the dipole and a very different relation outside the dipole. This is quite similar to $q-\psi$ plots for certain classes of dipole modon solutions of the BVE (Verkley 1993; Haines and Malanotte-Rizzoli 1991). The existence of a dipole region with a unique approximately linear $q-\psi$ relation is one of the criteria used to evaluate the nature of streamfunction fields in section 3.

Note that most $q-\psi$ plots have a distinct linear region associated with points at extreme polar latitudes that is not related to blocking events. This polar region is seen at the extreme left-hand side of Northern Hemisphere $q-\psi$ plots like Fig. 2 and can be seen in most of the $q-\psi$ plots displayed here.

c. *A forced barotropic vorticity equation*

Following the lead of PM and BrO, the relation of NSSs of (1) to the behavior of a forced, dissipative version of the BVE are examined here. The forced BVE of interest can be written in a form similar to that used in PM

$$\partial\nabla^2\psi/\partial t + J(\psi, q) = A\nabla^2(\psi - \psi_F),$$

where A is a linear operator whose diagonal elements are given by $\lambda(m, n)$. This can be rewritten for each component (symbolized by the subscripts m and n) of the discretized equation as

$$\partial\nabla^2\psi_{m,n}/\partial t + J(\psi, q)_{m,n} = \lambda(m, n)\nabla^2(\psi_{F_{m,n}} - \psi_{m,n}). \quad (4)$$

Here λ is a function of the spectral wavenumbers m and n in order to allow scale-selective forcing and dissipation. The forcing streamfunction, ψ_F, will be set to the NSS streamfunction for 14 January 1987, ψ_{NSS}, unless otherwise noted.

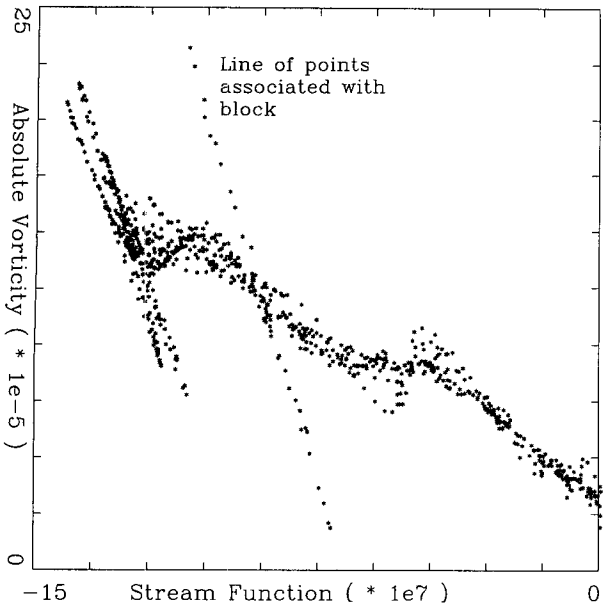

FIG. 2. Plot of absolute vorticity vs streamfunction ($q-\psi$ plot) corresponding to Fig. 1. Points are mostly confined to the Northern Hemisphere by plotting only those with streamfunction less than the global mean and positive vorticity.

A number of long integrations of (4) are discussed below. In all cases the integrations are performed using a third-order Adams–Bashforth time differencing scheme (Durran 1991) and a time step of 1800 s.

d. Blocking index

Although it is a sacrifice of precision for simplicity, any event in which the integration of (4) results in a strong high over low pattern over Europe with an accompanying distinct approximately linear relation between absolute vorticity and ψ will be referred to as a blocking event. It is not clear a priori that these events are in any way related to real blocks, although it is one purpose of this paper to begin to establish such a link.

To simplify the presentation of results, a single-valued measure of European blocking strength is required. A revised version of the measure of Lejenäs and Okland (1983) similar to that used in Anderson (1993) is applied here. The normalized blocking index B is specifically tailored to measure blocks in the European region of interest and is defined as

$$B = \max_{0E<K<25E} \left[\max_{41N<i<75N, i<j\leq 75N} (\psi_{j,k} - \psi_{i,k}) \right] / (3 \times 10^7), \tag{5}$$

where $\psi_{(i,j)}$ is the value of the streamfunction on the Gaussian grid corresponding to the spectral representation at latitude i and longitude j. Here B measures the largest area of midlatitude easterly flow between 0° and 25°E and is normalized to have a maximum value less than one for the experiment reported in section 3b.

3. Simulations of blocking behavior

This section examines several extended integrations of the forced BVE (4). Throughout this section, the forcing streamfunction is set to the NSS for 14 January 1987.

a. Vorticity forcing

The first version of (4) presented uses constant strength forcing, $\lambda(m, n) = \sigma$. This will be referred to as "vorticity" forcing since the right-hand side of (4) is just a relaxation toward the forcing vorticity field.

For all values of σ tested, vorticity forcing resulted in a value of the blocking index that was approximately constant throughout the integration. Examination of the integrated streamfunction fields shows that there is very little variance (compared to that found for other forcing types) in any frequency band for any value of σ. For $\sigma < 3 \times 10^{-6}$, the model produces flow that is nearly zonal over Europe, while for $\sigma > 4 \times 10^{-6}$, the flow over Europe is nearly indistinguishable from the NSS. For $3 \times 10^{-6} < \sigma < 4 \times 10^{-6}$, the value of the blocking index as a function of σ increases from less than zero (zonal flow) to approximately the same value as found for the NSS. However, there is never any significant variation of the index as a function of time within a given integration. For sufficiently large values of σ, the model reaches an exactly steady state.

Throughout this work, linear normal mode instability (Frederiksen 1983; Simmons et al. 1983), despite its many limitations, is used to evaluate some results of the extended integrations. In this case, (4) is linearized around both the high amplitude blocked time-mean streamfunction from the $\sigma = 4 \times 10^{-6}$ case and the low amplitude time mean from the $\sigma = 3 \times 10^{-6}$ case. When the model forced with $\sigma = 3 \times 10^{-6}$ is linearized around the low amplitude time mean, there is only a single very weakly unstable mode (e-folding time approximately 125 days). When the model forced with $\sigma = 4 \times 10^{-6}$ is linearized around the high amplitude basic state, there are no unstable modes. The almost total lack of linear instability is an explanation for the extremely limited variability found in the vorticity-forced model.

b. Thermal forcing

As noted in the introduction, one of the many potential explanations of blocking found in the literature is based on the interaction of transient "short waves" and low-frequency planetary waves. Observational support for blocks being the result of short wave energy conversion into stationary blocking patterns has been provided in Shutts (1986). In addition, there is theoretical evidence to support this view of blocking. Malguzzi

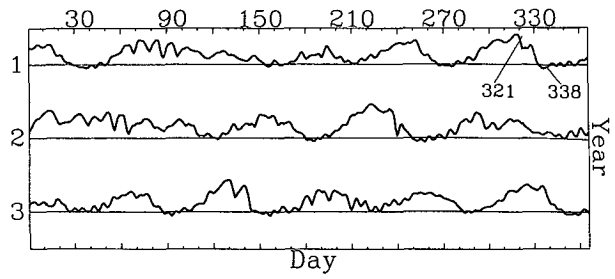

FIG. 3. Three-year time series of normalized blocking index B for thermal forcing toward the 14 January 1987 NSS, $\alpha = 7 \times 10^{-18}$. Horizontal lines are the zeros for each of the 3 years.

(1993) shows that a highly truncated barotropic system can display behavior in which short waves interact with large-scale waves to produce structures resembling blocks. Haines and Marshall (1987) showed that a source of eddies was needed to maintain blocklike modon structures in a quasigeostrophic beta-plane model. The approach of Shutts (1983) is based on a distinct but similar line of reasoning. Again, a large-scale diffluent flow provides the potential for blocking, and short waves provide the catalyst to initiate a blocking event.

These results, and the stability analysis of the previous subsection, suggest that applying a scale-selective forcing in (4) has potential to produce results that are more closely related to the behavior of actual blocks. In order to continue to strongly force long waves while allowing short waves to grow and propagate relatively freely, the forcing function is set to

$$\lambda(m, n) = -\alpha a^2/n(n + 1). \qquad (6)$$

Here, α is a constant, and a is the radius of the earth. Equation (4) then becomes

$$\partial\nabla^2\psi/\partial t + J(\psi, q) = \alpha(\psi - \psi_F). \qquad (7)$$

This forcing will be referred to as thermal forcing since the right-hand side of (7) can be viewed as a thermal forcing in a shallow-water model context.

Again, a number of long integrations for different values of α in (7) have been examined. For $\alpha < 4 \times 10^{-18}$, the results are similar to the weak ($\sigma < 3 \times 10^{-6}$) vorticity forcing cases; the flow is approximately zonal, the blocking index remains negative, and there is relatively little variation of ψ within an individual integration. Similarly, for $\alpha > 1.2 \times 10^{-17}$, the flow is always blocked and similar to the NSS although there is much more variability on timescales of several days than in the vorticity-forced cases. In this thermal-forcing case, however, there exists an intermediate range of α for which the integrations develop behavior with significant high and low frequency variability that is qualitatively similar to observed atmospheric flows.

Figure 3 displays the blocking index B for a three-year segment in the middle of an extended 10 000-day integration of (7) with $\alpha = 7 \times 10^{-18}$. The blocking index reveals extended periods of blocked behavior (high B) interspersed with relatively zonal flow periods (B close to zero). Both the blocks and the zonal flow periods tend to have lifetimes on the order of 20 days. This behavior is somewhat realistic and is certainly comparable in simulation quality to behavior demonstrated in other simple models (PM, Shutts 1983).

Figure 4 displays the distribution of the daily blocking index values from the 10 000 day run. The distribution appears to be significantly skewed suggesting that some degree of regimelike behavior with rapid transitions between blocked and zonal states is occurring in the model (Reinhold and Pierrehumbert 1982; Vautard et al. 1988). Although the distribution is suggestive of bimodality, no statistical test of this is offered here; there seems to be continuing discussion in the atmospheric literature about the best way to evaluate the significance of such distributions (Nitsche et al. 1994). However, the distribution appears to be at least as bimodal as the best of the heavily processed observed atmospheric distributions that have been claimed to be bimodal (Dole and Gordon 1983; Hansen and Sutera 1991); similarly skewed distributions are found for other regimelike cases discussed below.

The blocked and zonal states in the integration can be shown to be dynamically distinct. Figure 5 displays streamfunction fields for representative blocked and zonal flow states (marked on the time series of Fig. 3) from the long integration. The blocked state, Fig. 5a, shows a distinct dipole structure over Europe, while the zonal state, Fig. 5b, has only a weak diffluent flow in

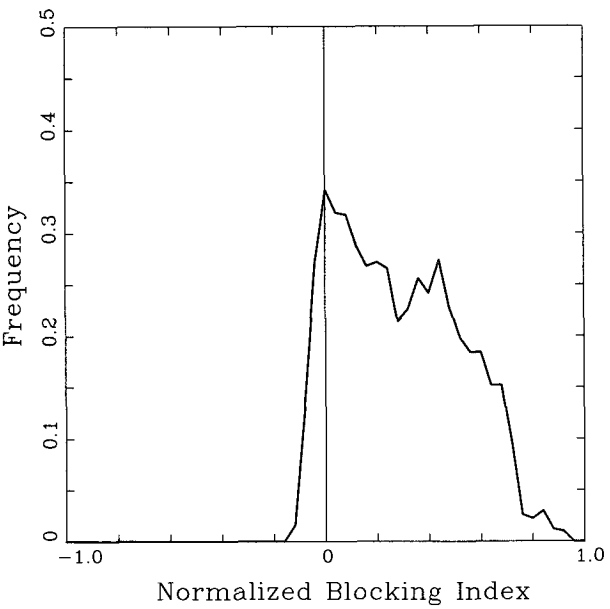

FIG. 4. Distribution of normalized blocking index from 10 000 daily values for thermal forcing toward 14 January 1987 NSS, $\alpha = 7 \times 10^{-18}$.

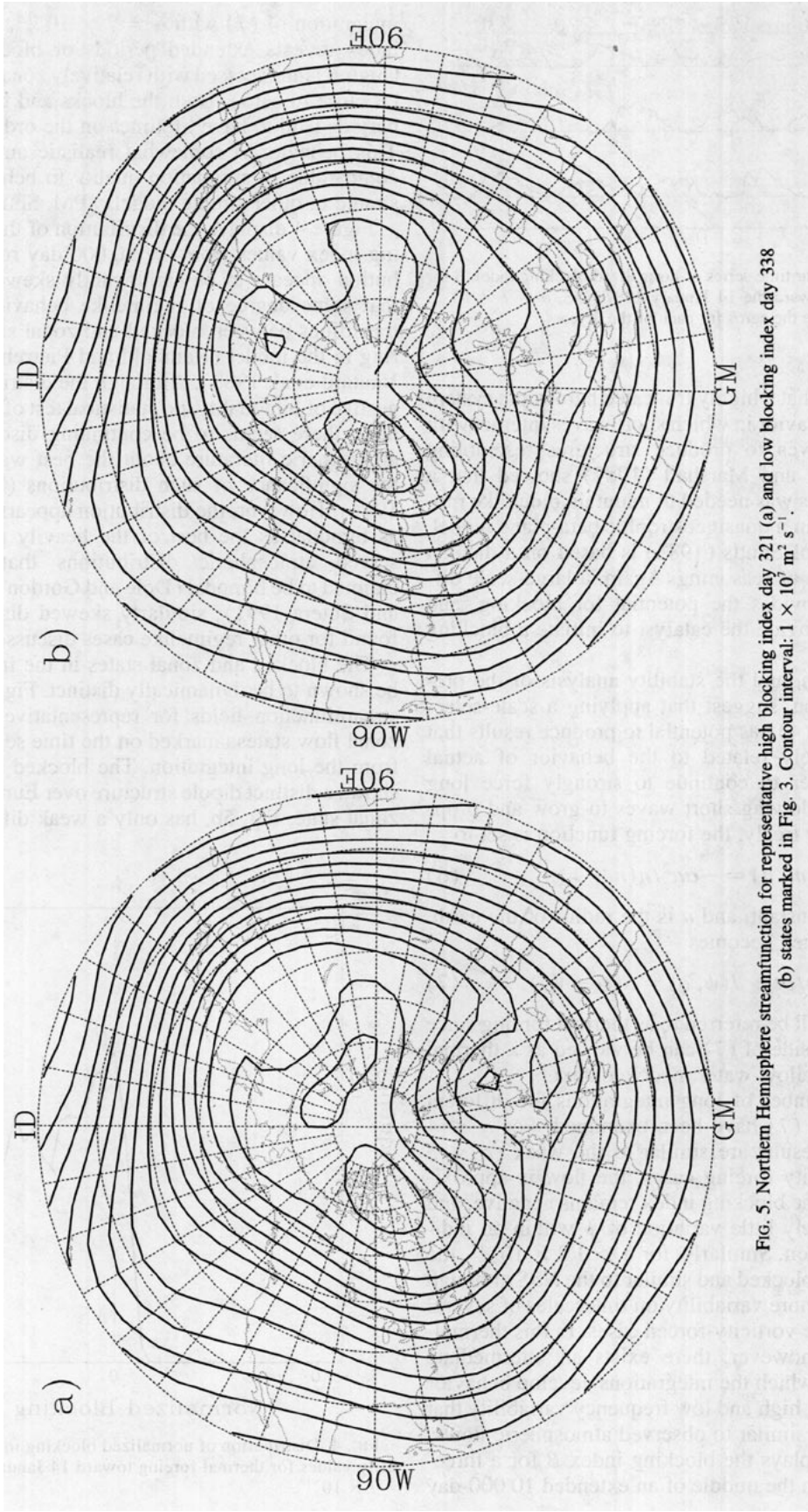

FIG. 5. Northern Hemisphere streamfunction for representative high blocking index day 321 (a) and low blocking index day 338 (b) states marked in Fig. 3. Contour interval: 1×10^7 m^2 s^{-1}.

this region with no evidence of reverse flow or closed circulations. These states can be compared, for example, to those shown in PM, which are considerably less distinct.

The $q-\psi$ plots for the streamfunctions in Fig. 5 are also distinct. Figure 6a shows the $q-\psi$ plot corresponding to the blocked state in Fig. 5a. Although the highlighted points from the blocking region are not as close to linear as those in Fig. 2, they are clearly distinct from the points in the surrounding relatively zonal flow. The $q-\psi$ plot for the zonal state, Fig. 6b, shows no such distinct region.

The streamfunction field in the vicinity of the block also displays surprisingly realistic evolution. Animation of streamfunction fields during block formation or decay are qualitatively similar to observed events although the strength of the transient short waves is less than is observed in the real atmosphere. In fact, recent experimentation with a similar forced model has shown that barotropic models are able to do a surprisingly accurate job in representing the evolution of strong observed blocking events from 2-day and 4-day precursors.

Figure 7 shows the high-pass and low-pass standard deviations of ψ for the $\alpha = 7 \times 10^{-18}$ integration. The Haming filter of Blackmon (1976) is used to filter twice daily time series. Following many observational studies (Lau 1979; Nakamura and Wallace 1991), the high-frequency fields emphasize periods between 2.5 and 6 days, while the low-frequency filter keys on periods between 10 and 90 days. The majority of the low-pass variability (Fig. 7a) is in the region of the European block and another blocking region north of Asia. This additional block is also seen in the NSS, but is ignored throughout the discussion here since it is apparently dynamically distinct from the European block. In fact, if the forcing basic states are modified to be more zonal over this second region, no blocking behavior occurs there while the behavior of the European blocking region is unchanged. The high-pass variability (Fig. 7b) is confined generally to the Pacific sector in a "barotropic storm track."

Again, linear instability can be used to help interpret the results. In this case, (7) is linearized around the blocked time-mean flow of the $\alpha = 1.2 \times 10^{-17}$ integration and the approximately zonal time-mean flow of the $\alpha = 4 \times 10^{-18}$ integration. When linearized around the low-amplitude zonal flow, the model forced with $\alpha = 7 \times 10^{-18}$ has two significantly unstable modes [e-folding time O(10) days], one confined to extreme polar latitudes, and the other in the form of an eastward propagating midlatitude wave.

When linearized about the blocked time mean, the model forced with $\alpha = 7 \times 10^{-18}$ has five significantly unstable modes. Four of these have corresponding eigenvectors with amplitude confined to the region of the European block or the other Northern Hemisphere block (there is also amplitude in the vicinity of a Southern Hemisphere block that is not discussed here). The fifth unstable mode is similar to the midlatitude unstable mode found for the zonal basic state.

These results suggest that the significantly enhanced variability of the thermal forcing compared to the vorticity forcing model is partially due to the presence of

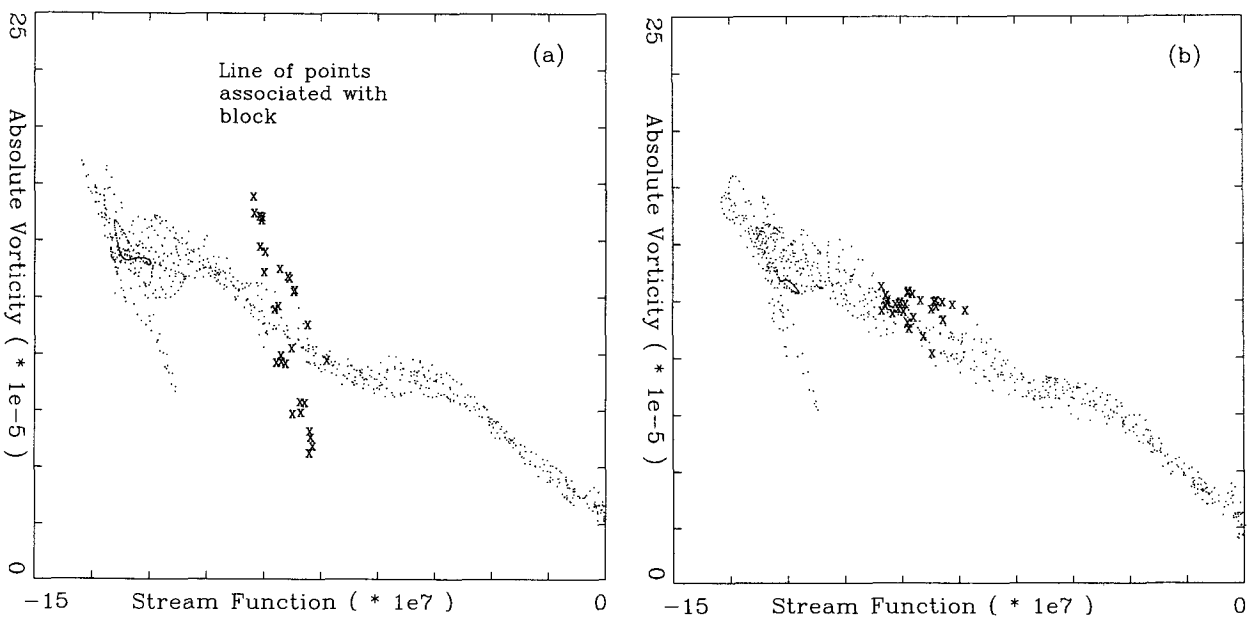

FIG. 6. Plot of $q-\psi$ corresponding to streamfunction fields in Fig. 5. Points from the blocking region, longitude from 0° to 40°E and latitude from 40° to 70°N, are marked by "X" and all other points by dots.

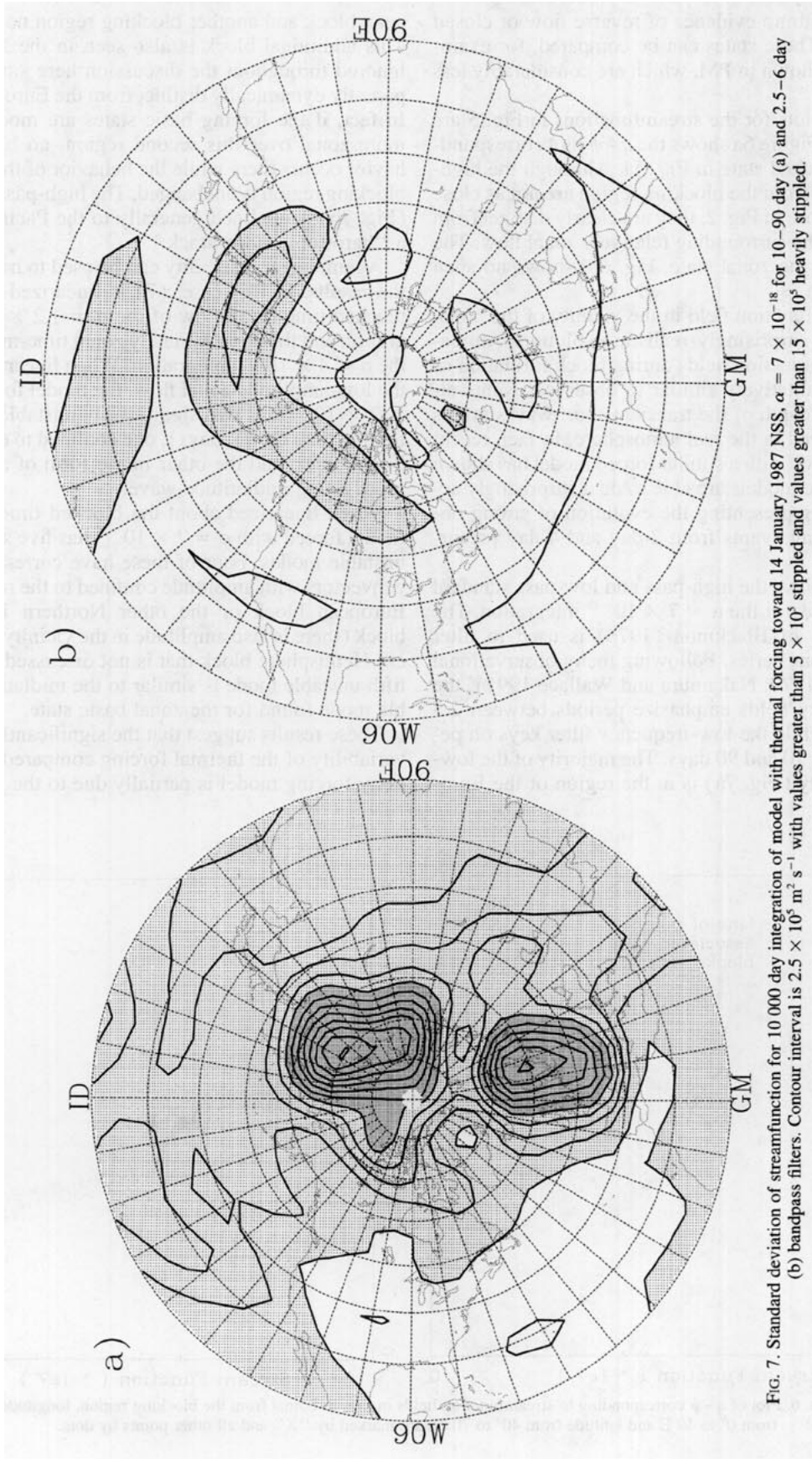

FIG. 7. Standard deviation of streamfunction for 10 000 day integration of model with thermal forcing toward 14 January 1987 NSS, $\alpha = 7 \times 10^{-18}$ for 10–90 day (a) and 2.5–6 day (b) bandpass filters. Contour interval is 2.5×10^5 m^2 s^{-1} with values greater than 5×10^5 stippled and values greater than 15×10^5 heavily stippled.

linear instabilities. In the thermal forcing case, the large-scale waves can be forced hard enough to provide a "realistic" time-mean basic state while still leaving shorter waves free enough to allow transients to result through instability.

The results presented in this subsection are from a model with no explicit parameterized diffusion. A discussion of the impacts of including diffusion is presented in section 5a.

c. *Scale-selective forcing*

The analysis at the end of the previous section suggests that by further reducing the forcing of the short waves, while continuing to strongly force the long waves, even more variability might result. Chen and Juang (1992) have demonstrated this hypothesis in a GCM by artificially increasing model transient strength and observing an increase in blocking frequency. To verify this hypothesis, the model was integrated with the thermal forcing as in (7) for spectral waves with $n \leq 10$ and $|m| \leq 4$, and no forcing for all other waves. In addition, a ∇^8 diffusion is added to the scale-selective streamfunction forcing experiment making the complete model equation

$$\partial\nabla^2\psi/\partial t + J(\psi, q) = \alpha(\psi - \psi_F) - \kappa\nabla^8\zeta. \quad (8)$$

Unless otherwise noted, the damping strength, κ, in all the scale-selective forcing experiments that follow is selected so that the smallest resolved wave is damped with a 10-day timescale.

This experiment exhibits behavior that is qualitatively similar to that exhibited by the unmodified thermal forcing experiments of the previous subsection. For an intermediate range of forcing strength α, interesting behavior ensues with blocks interspersed with zonal flows. The blocks tend to be even stronger than those found in the unmodified case, and there is considerably more high-frequency variability. Examination of an animation of the streamfunction field shows that much stronger short waves propagate on the approximately zonal flow outside the blocking region, and some of these strong short waves significantly modify the structure of even persistent blocks as they propagate through the blocking region.

Figure 8 shows a 3-year segment of the blocking index for $\alpha = 1.4 \times 10^{-17}$ and forcing confined to $n \leq 10$ and $|m| \leq 4$. A number of "blocking" events with lifetimes O(10) days can be seen. There is much more high-frequency variability than in Fig. 3 due to the impact of much higher-amplitude transient short waves on the blocking index.

Figure 9 shows the bandpass filtered standard deviation for the scale-selective thermal forcing. The low-frequency variability (Fig. 9a) in the extratropics is higher in the blocking region as in Fig. 7. There is considerably enhanced low-frequency variability in the Tropics south of 30°N; this is associated with very low-frequency shifts of the "barotropic" jet streams. These shifts occur at considerably lower frequencies than most of the blocking behavior and do not seem to be dynamically related to the blocks.

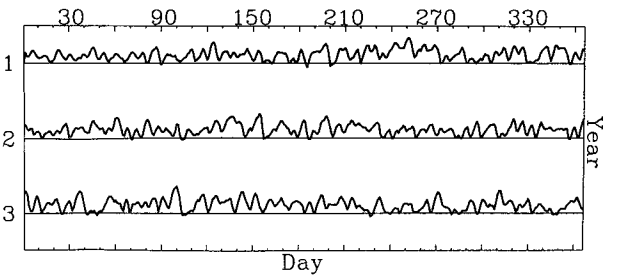

FIG. 8. As in Fig. 3 but for $n \leq 10$, $|m| \leq 4$ thermal forcing toward 14 January 1987 NSS, $\alpha = 1.4 \times 10^{-17}$.

The high-frequency variability (Fig. 9b) is enhanced throughout the hemisphere compared to that in Fig. 7b. Centers of high-frequency variance stretch from eastern Asia into the Pacific and across North America. Additional low-latitude centers also exist. These are "wave guides" for barotropic transient short waves. The North American "storm track" weakens over the Atlantic, and the extreme end appears to curve north around the European blocking region, which displays a relative minimum of high-frequency variance. Both the high and low frequency variance and the life cycles of blocking events are qualitatively similar in many respects to that observed in some Januaries.

4. NSSs and regimelike behavior

This section will explore the relation between NSSs and the regimelike blocking behavior discussed in the last section. For the purposes of this paper, "regimelike" is defined as the existence of blocking/zonal flow events with lifetimes considerably greater than the period of the small-scale transient waves found in the model. This is similar to definitions of regimes that have been used in observational studies. Both the blocking time series plots and the bandpass standard deviation of the streamfunction can demonstrate the existence of regimelike behavior under this definition.

So far, only limited evidence relating NSSs of the BVE to the existence of regimelike behavior has been presented. It is quite conceivable that forcing the BVE toward an observed (not NSS) streamfunction with a high amplitude block, or even a weak split flow, would result in regimelike behavior for the appropriate values of forcing strength. This would be consistent with the theoretical study of Malguzzi (1993), where all that is required is the interaction between a large-scale diffluent region and small-scale transient waves.

In fact, the results of section 3c demonstrate that *forcing* toward an NSS is not necessarily a prerequisite for producing regime-like behavior. When truncated to

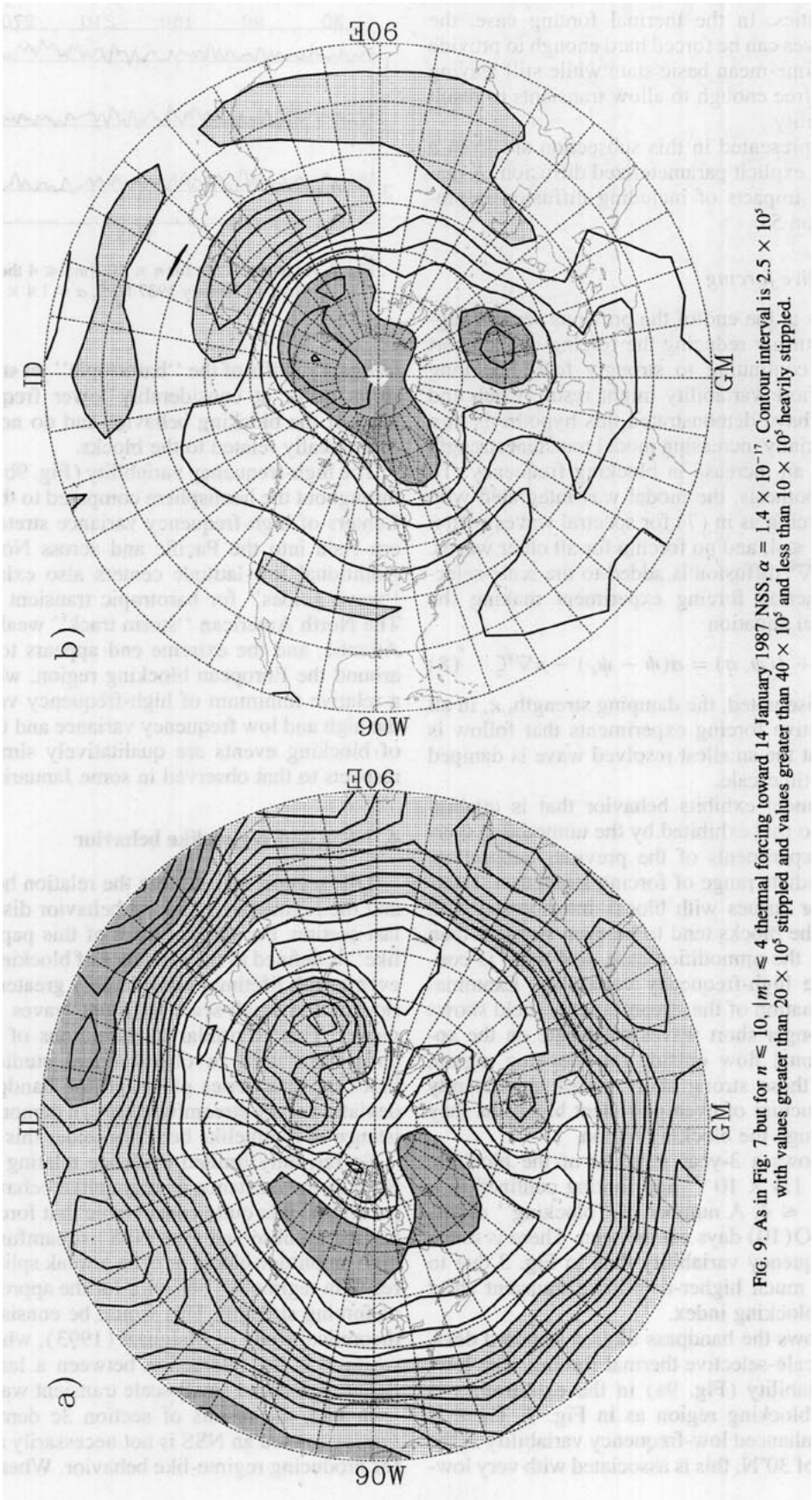

FIG. 9. As in Fig. 7 but for $n \leq 10$, $|m| \leq 4$ thermal forcing toward 14 January 1987 NSS, $\alpha = 1.4 \times 10^{-17}$. Contour interval is 2.5×10^5 with values greater than 20×10^5 stippled and values greater than 40×10^5 and less than 10×10^5 heavily stippled.

$n \leq 10$, $|m| \leq 4$, the 14 January 1987 NSS acquires a significant time tendency several orders of magnitude greater than the NSS but still several orders less than the observed state.

Actually, the spectrally truncated NSS streamfunction does not explicitly contain any dipole structure. Figure 10 shows the $q-\psi$ plot for the truncated NSS. There is no evidence of a distinct linear $q-\psi$ relation associated with a blocking region. Despite this, the extended integration of (8) forced toward the truncated NSS clearly generates dipole blocking structures.

Forcing (8) toward the observed 14 January 1987 streamfunction with scale-selective ($n \leq 10$, $|m| \leq 4$) thermal forcing (this case is referred to hereafter as SSψOBS) also produces regimelike behavior, qualitatively similar to that reported in section 3c. Like the NSS, the observed 14 January 1987 flow truncated to $n \leq 10$, $|m| \leq 4$ has no evidence of a blocking NSS in its $q-\psi$ plot (not shown).

Nevertheless, there is still substantial evidence that NSSs are playing an important role in the generation of regimelike behavior. Figure 11 shows the $q-\psi$ plot for a strongly blocked state from the middle of the SSψOBS experiment with $\alpha = 1.4 \times 10^{-17}$. There is a distinct region (highlighted in the plot) associated with a strong block over Europe. Although there is considerably more scatter in the highlighted region than was seen in the NSS $q-\psi$ plot of Fig. 2, the highlighted points are still fairly well approximated by a line with slope similar to that seen in Fig. 2. There is no evidence of this quasi-linear region in $q-\psi$ plots for low blocking index days in this experiment. Even though the *forcing* does not explicitly contain such a region, the forced integration periodically visits a high amplitude state that is very similar to a blocked NSS. The appearance of this blocking NSS structure argues that it is the existence of NSSs in the model's phase space that results in the unusual persistence of blocking events.

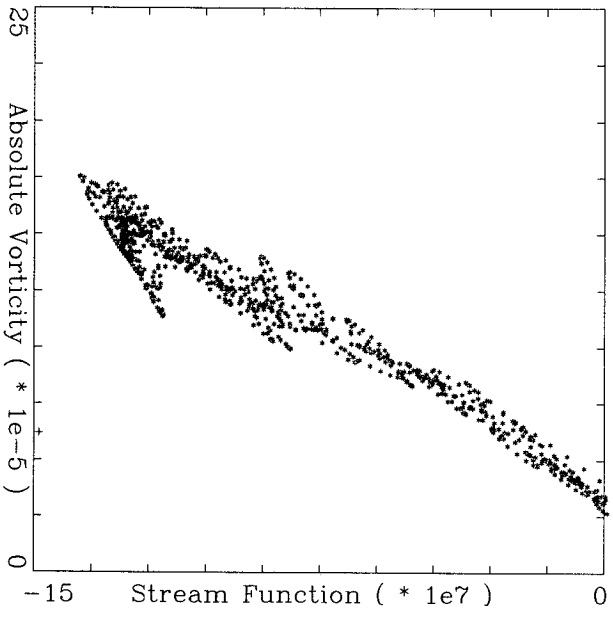

FIG. 10. Plot of $q-\psi$ for 14 January 1987 NSS truncated to contain only spectral components with $n \leq 10$ and $|m| \leq 4$.

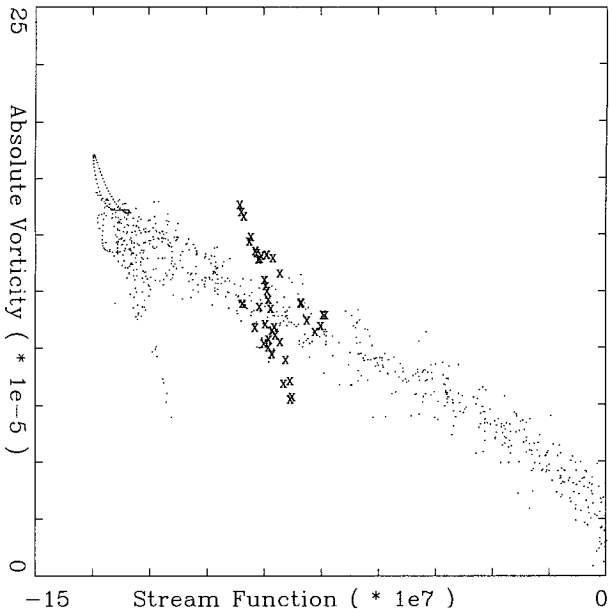

FIG. 11. Plot of $q-\psi$ for strongly blocked state in SSψOBS integration ($n \leq 10$, $|m| \leq 4$ thermal forcing toward 14 January 1987 observations). Points from the blocking region are highlighted as in Fig. 6.

Additional evidence that NSSs are influencing the regimelike behavior can be found by constructing NSSs of the SSψOBS model [(8) with only $n \leq 10$, $|m| \leq 4$ forced toward the 14 January 1987 observations]. Figure 12 shows the $q-\psi$ plots for NSSs of the SSψOBS model that are close to a blocked state and a zonal state from the extended integration. It appears that the forced equation has two distinct classes of NSSs, one blocked (Fig. 12a) and one relatively zonal (Fig. 12b), and that these NSSs appear to be related to the two "regimes" of the model integration.

Recall that the unforced BVE also possessed at least two classes of NSSs, one exactly zonal and one blocked, but does not exhibit regimelike behavior when integrated. There are two reasons for the lack of observable blocking behavior in the free BVE. First, although the large amplitude dipole NSSs of the free BVE have very small time tendency, they break down rapidly [O(10) days] through linear instability, and the free BVE is never again able to generate sufficient wave amplitude to return to the vicinity of the NSS (this is a result of the cascade of energy to large scales in the unforced BVE). Second, there is nothing in the free BVE to break the longitudinal symmetry. There-

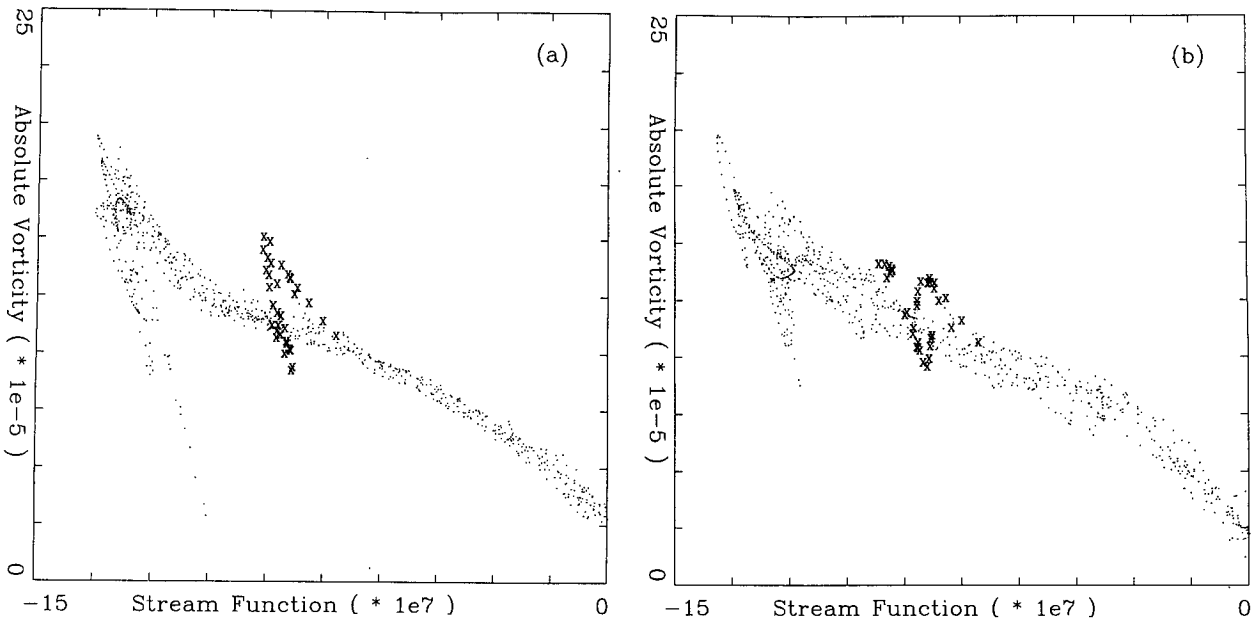

FIG. 12. Plot of $q-\psi$ for NSSs of the SSψOBS model that are close to a blocked state (a) and a nearly zonal state (b) of the extended model integration. Points from the blocking region are highlighted as in Fig. 6.

fore, there exists a dipole NSS at each longitude. It becomes difficult to diagnose any small amplitude effects of NSSs in this case since resulting blocks could occur at any longitude.

Things are quite different in forced BVEs like (8). The blocked NSS occurs in a unique longitudinal position, so it is easier to detect. In addition, the forcing acts to keep the model integration close enough to the blocking state that it is able to recur (one can also view the forcing as providing an energy source for the small scales needed to produce blocking). This combination appears to allow the blocked and zonal NSSs to produce the distinctive blocking behavior found in the forced model runs.

5. Additional results

a. Sensitivity to diffusion

The regimelike behavior observed in the last two sections can be quite sensitive to the strength of the ∇^8 diffusion term in (8). Figure 13 shows time series for 365 days of integrations of the scale-selective streamfunction forcing with $\alpha = 1.4 \times 10^{-17}$ as the diffusion is varied. The diffusion is measured in terms of the damping time for the smallest (most strongly damped) waves, with results shown for no diffusion, 5-day, and 2-day damping. The case with no diffusion has very strong blocks and a great deal of high-frequency variability. As diffusion is increased, the high frequencies become progressively smaller and the maximum blocking strength progressively weaker. By the time a 2-day diffusion is reached, the blocking index time series shows a uniformly zonal flow with regular weak high-frequency waves.

This behavior can be partially explained using the linear normal modes of the model (8) linearized around a blocked or a zonal flow from the extended integration. For the case with no diffusion, both linear problems have more than 30 unstable modes with many having e-folding times of approximately 5 days. As the diffusion is increased, the number of unstable modes decreases rapidly for the case linearized around the zonal flow, and less rapidly for the case linearized around blocked flow. By the time the 2-day diffusion is reached, each has approximately eight unstable modes, but the smallest e-folding time for the zonal flow case is more than 10 days. This lack of strong linear instability may explain the significantly reduced amplitude of high-frequency transients and the resulting lack of regime-like blocking behavior.

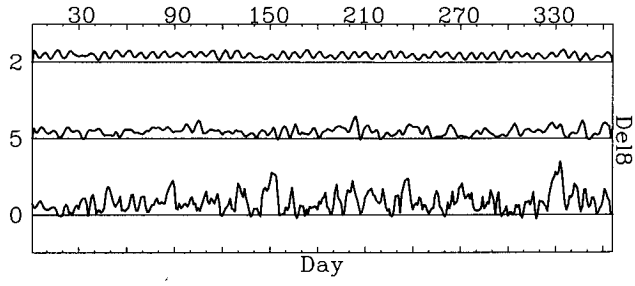

FIG. 13. One-year segments of normalized blocking index B for the same forced model as in Fig. 8 but with 2 day and 5 day ∇^8 diffusion and no diffusion (labeled 0).

It is difficult to choose the appropriate strength for diffusion in any model, especially an idealized one. Here, the spectra of the model's energy and enstrophy as a function of total wavenumber were examined. In accordance with both observational (Boer and Shepherd 1983) and theoretical (Leith 1968) results, the strength of the ∇^8 diffusion was adjusted so as to best approximate a -3 power law for the energy. In the scale-independent thermal forcing results of section 3b, the forcing itself acts to constrain the energy at all scales. The slope of the energy spectrum is very close to -3 without the addition of any diffusion. Adding significant ∇^8 diffusion steepens the energy slope and results in a much reduced variability in the model.

For the scale-selective $n \leq 10$, $|m| \leq 4$ case of section 3c, a value of 10 days for the diffusive timescale acting on the smallest resolved wave gave a spectral slope close to -3. A model with no diffusion had a slope closer to -2.5, and a 2-day ∇^8 produced a slope close to -3.5. The 10-day diffusion on the smallest resolved scale was also found to give slopes near -3 for model resolutions different from T21 and was included in all high-resolution runs discussed in the next subsection.

b. *Sensitivity to resolution*

The behavior of the forced model is also sensitive to model truncation. A number of cases have been run at T42, and a few at T63 resolution. An example of a blocking index time series for a $n \leq 10$, $|m| \leq 4$ thermal forced, $\alpha = 1.4 \times 10^{-17}$, T42 integration is shown in Fig. 14. This case is forced toward a T42 NSS, which is generated by applying the unforced NSS minimization at T42 to the T21 NSS. The $q-\psi$ plots for individual blocked cases have distinct linear regions, whereas the more zonal cases do not. Truncation T42 results are not quite as sensitive to the introduction of ∇^8 diffusion as are T21 results.

Blocking behavior has also been found in T63 versions of (8). Figure 15 shows a time series of the blocking index for a T63 model forced toward the T21 14 January NSS for $n \leq 10$, $|m| \leq 4$ with $\alpha = 1.4 \times 10^{-17}$. There are a number of high index events with lifetimes about 10 days as well as long periods without significant high amplitude events. Figure 16 displays the streamfunction for a high index day and a low index day from the third year of the T63 integration. The high index day has a high over low structure over Europe, while the low index day is relatively zonal. The corresponding $q-\psi$ plots have a distinct quasi-linear region associated with the block for the high index day, but not for the low index day.

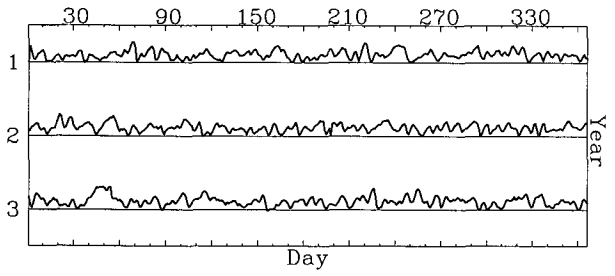

FIG. 14. As in Fig. 3 but for T42 model with $n \leq 10$, $|m| \leq 4$ thermal forcing toward a T42 NSS for 14 January 1987, $\alpha = 1.4 \times 10^{-17}$.

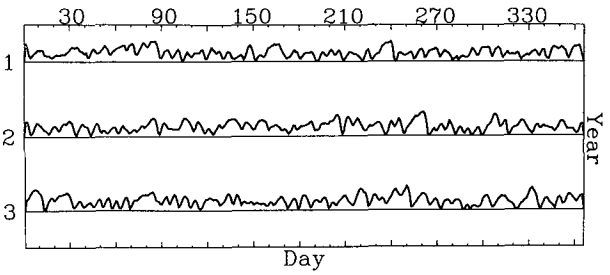

FIG. 15. As in Fig. 3 but for T63 model with $n \leq 10$, $|m| \leq 4$ thermal forcing toward the T21 NSS for 14 January 1987, $\alpha = 1.4 \times 10^{-17}$.

6. Discussion

An attempt has been made to unify two possible explanations of blocking in the context of the BVE on the sphere. In accord with the first explanation, the existence of both zonal and blocked nearly stationary states of the unforced BVE suggested that these NSSs might be related to the observed regimelike behavior of the real atmosphere. However, the unforced BVE never returns to a recognizably blocked state when integrated. In addition, the unforced BVE is zonally symmetric, so there is no reason for a block to form more frequently at any particular longitude.

A forced BVE was constructed to overcome these difficulties; this is a natural step since the long waves of the observed Northern Hemisphere winter are not zonally symmetric due to the effects of inhomogeneous land surface and orographic forcing. The original forced BVE was specifically designed to have a longitudinally fixed blocking NSS when forced toward a blocked NSS of the unforced BVE.

Introducing the forcing in the most obvious way ("vorticity" forcing) proved to be insufficient to produce regimelike behavior. At this point, it became necessary to make use of ideas from a second explanation of blocking. Observational and model studies had suggested that the interaction between transient high-frequency waves and diffluent low-frequency long waves could result in blocked flow. An analysis of the original forced BVE demonstrated that it had very little transient short-wave amplitude. Reducing the strength of the forcing applied to short waves, while maintaining

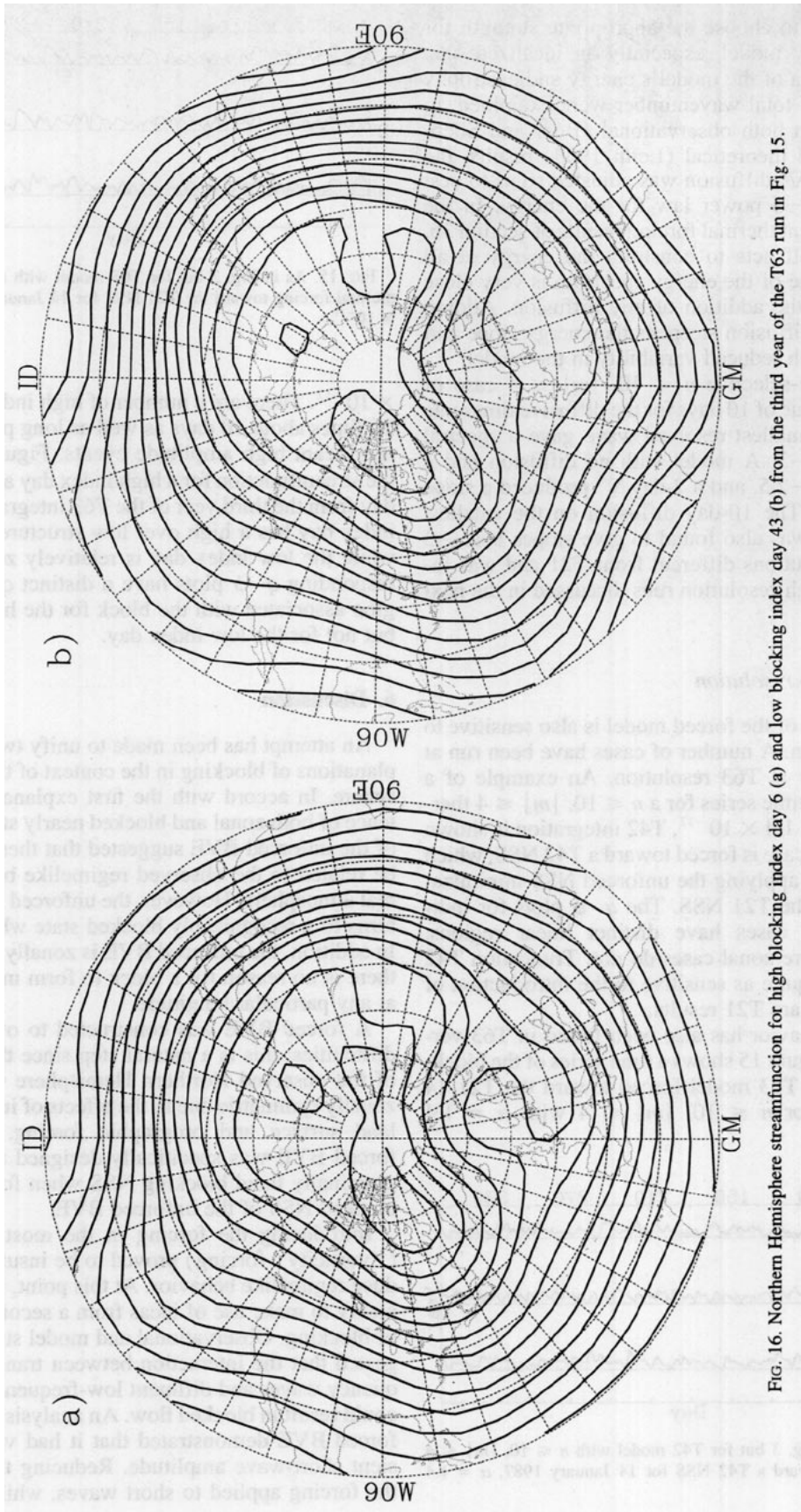

FIG. 16. Northern Hemisphere streamfunction for high blocking index day 6 (a) and low blocking index day 43 (b) from the third year of the T63 run in Fig. 15.

a strongly forced diffluent long-wave pattern (thermal forcing) offered a chance to alleviate this problem. The result was regimelike blocking behavior in a forced BVE on the sphere.

One possible interpretation of the results is as follows: the existence of multiple regimes in the forced BVE is related to the existence of corresponding NSSs. This is essentially an extension of the beta-plane theory of Reinhold and Pierrehumbert (1982) to a less severely truncated model on the sphere. As in Reinhold and Pierrehumbert, relatively strong transient short waves are needed to "push" the system from one regime to another. Reinhold and Yang (1993) studied similar transition mechanisms in more idealized models. In the "vorticity" forced model, all scales are forced toward the NSS, thus precluding the existence of any strong transients.

In order to produce strong transients, the damping on the short-wave components must be reduced or eliminated. At the same time, long-wave components must be forced for two reasons. First, the long-wave forcing keeps the system somewhere close to the appropriate NSSs in phase space. Second, the forced long waves provide an energy source for short-wave transients through barotropic instability.

Weak forcing results in a perpetually zonal flow because the source of short-wave energy is too small or the model is too far from a blocking NSS. Excessively strong forcing results in a perpetually high amplitude state with very strong transients. Such a state might be viewed as perpetually blocked although the strong transients mask the signatures of blocking in fields that are not time averaged.

The end result is that the forced barotropic blocking mechanism proposed here is quite sensitive to changes in parameters. For instance, the addition of small amounts of diffusion apparently reduces transient short-wave energy enough to reduce the strength and number of regime transitions.

The hypothetical mechanism just outlined could have been proposed without the mention of stationary states simply using the concept of transient interaction with a forced diffluent long-wave background flow. Evidence was presented, however, that dipole NSSs are intimately related to the behavior observed in the forced model. In the $n \leq 10$, $|m| \leq 4$ forcing case, the forcing streamfunction is no longer a particularly good NSS, and it certainly contains no explicit dipole. In addition, cases in which the BVE was forced toward the $n \leq 10$, $|m| \leq 4$ observed flow (SSψOBS), which also has no explicit dipole, were examined. In both cases, however, the model exhibits regimelike behavior, which includes blocked states that are similar to and close to dipole NSSs. Although not conclusive, this strongly suggests that the existence of dipole NSSs of the forced BVE are playing a part in the regimelike behavior.

7. Conclusions

A forced version of the barotropic vorticity equation that can produce a reasonable simulation of observed blocking behavior has been described. In addition to producing regimelike episodes of zonal and blocked flow, the model produces surprisingly realistic patterns of low and high frequency variance. A possible mechanism explaining the forced model behavior suggests that nearly stationary states of the forced model are responsible for the existence of the two distinct regimes. Transient short waves are responsible for "pushing" the model from one regime to another.

The fact that a purely barotropic model can simulate blocking suggests that barotropic dynamics might play a dominant role in real atmospheric blocking. There exists observational evidence to support the hypothesis that barotropic dynamics may dominate atmospheric blocking behavior (Nakamura and Wallace 1993). Atmospheric blocking regimes could be related to NSSs of the "real" governing equations that are similar to NSSs of the BVE. Atmospheric transient short waves could act, presumably through predominantly barotropic processes, to push the atmosphere from blocked to zonal flow regimes. Obviously, the source of transient waves in the real atmosphere is not predominantly barotropic instability. This might make the atmospheric mechanism considerably more robust than the purely barotropic mechanism discussed here in which the background diffluent-flow forcing is also directly linked to the strength of the barotropic short waves.

A great deal of additional research is still needed to understand the dynamics of the blocking mechanism in spherical numerical models. A more careful analysis of the interaction between the background diffluent flow and transients in forced barotropic models is needed. Adding a "wave maker" to force small-scale transient short waves would allow more controlled experiments by liberating the transient wave source from instability of the background flow. A search for similar regimelike behavior in multilevel models is also of interest.

Acknowledgments. The author is indebted to Isaac Held, Vitaly Larichev, Grant Branstator, and three anonymous reviewers, who have all made significant contributions to this work.

REFERENCES

Anderson, J. L., 1992: Barotropic stationary states and persistent anomalies in the atmosphere. *J. Atmos. Sci.*, **49**, 1709–1722.

——, 1993: The climatology of blocking in a numerical forecast model. *J. Climate*, **6**, 1041–1056.

Benzi, R., A. R. Hansen, and A. Sutera, 1984: On stochastic perturbation of simple blocking models. *Quart. J. Roy. Meteor. Soc.*, **110**, 393–409.

——, S. Iarlori, G. Lippolis, and A. Sutera, 1988: Steady nonlinear response of a barotropic quasi-nondimensional model to complex topography. *J. Atmos. Sci.*, **45**, 3313–3319.

Blackmon, M. L., 1976: A climatological spectral study of 500 mb geopotential height of the Northern Hemisphere. *J. Atmos. Sci.*, **33**, 1607–1623.

Boer, J. G., and T. G. Shepherd, 1983: Large-scale two-dimensional turbulence in the atmosphere. *J. Atmos. Sci.*, **40,** 164–184.

Branstator, G., and J. D. Opsteegh, 1989: Free solutions of the barotropic vorticity equation. *J. Atmos. Sci.*, **46,** 1799–1814.

Butchart, N., K. Haines, and J. C. Marshall, 1989: A theoretical and diagnostic study of solitary waves and atmospheric blocking. *J. Atmos. Sci.*, **46,** 2063–2078.

Charney, J. G., and J. G. DeVore, 1979: Multiple flow equilibria in the atmosphere and blocking. *J. Atmos. Sci.*, **36,** 1205–1216.

Chen, W. Y., and H.-M. H. Juang, 1992: Effects of transient eddies on blocking flows: General circulation model experiment. *Mon. Wea. Rev.*, **120,** 787–801.

Dole, R. M., and N. D. Gordon, 1983: Persistent anomalies of the extratropical Northern Hemisphere wintertime circulation: Geographical distribution and regional persistence characteristics. *Mon. Wea. Rev.*, **111,** 1567–1586.

Durran, D. R., 1991: The third-order Adams–Bashforth method: An attractive alternative to leapfrog time differencing. *Mon. Wea. Rev.*, **119,** 702–720.

Frederiksen, J. S., 1983: A unified three-dimensional instability theory of the onset of blocking and cyclogenesis. Part II: Teleconnection patterns. *J. Atmos. Sci.*, **40,** 2593–2609.

Haines, K., and J. Marshall, 1987: Eddy-forced coherent structures as a prototype of atmospheric blocking. *Quart. J. Roy. Meteor. Soc.*, **113,** 681–704.

——, and P. Malanotte-Rizzoli, 1991: Isolated anomalies in westerly jet streams: A unified approach. *J. Atmos. Sci.*, **48,** 510–526.

Hansen, A. R., and A. Sutera, 1991: Planetary-scale flow regimes in midlatitudes of the Southern Hemisphere. *J. Atmos. Sci.*, **48,** 952–964.

Hoskins, B. J., 1973: Stability of the Rossby–Haurwitz wave. *Quart. J. Roy. Meteor. Soc.*, **99,** 723–745.

Lau, N.-C., 1979: The structure and energetics of transient disturbances in the Northern Hemisphere wintertime circulation. *J. Atmos. Sci.*, **36,** 982–1016.

Leith, C. E., 1968: Diffusion approximation for two-dimensional turbulence. *Phys. Fluids,* **11,** 671–673.

Lejenäs, H., and H. Økland, 1983: Characteristics of Northern Hemisphere blocking as determined from a long time series of observational data. *Tellus,* **35A,** 350–362.

Malguzzi, P., 1993: An analytical study on the feedback between large- and small-scale eddies. *J. Atmos. Sci.*, **50,** 1429–1436.

Nakamura, H., and J. M. Wallace, 1991: Skewness of low-frequency fluctuations in the tropospheric circulation during Northern Hemisphere winter. *J. Atmos. Sci.*, **48,** 1441–1448.

——, and ——, 1993: Synoptic behavior of baroclinic eddies during the blocking onset. *Mon. Wea. Rev.*, **121,** 1892–1903.

Neven, E. C., 1992: Quadrupole modons on a sphere. *Geophys. Astrophys. Fluid Dyn.*, **65,** 105–126.

Nitsche, G., J. M. Wallace, and C. Kooperberg, 1994: Is there evidence of multiple equilibrium in planetary wave amplitude statistics? *J. Atmos. Sci.*, **51,** 314–322.

Pierrehumbert, R. T., and P. Malguzzi, 1984: Forced coherent structures and local multiple equilibria in a barotropic atmosphere. *J. Atmos. Sci.*, **41,** 246–257.

Read, P. L., P. B. Rhines, and A. A. White, 1986: Geostrophic scatter diagrams and potential vorticity dynamics. *J. Atmos. Sci.*, **42,** 3226–3240.

Reinhold, B. B., and R. T. Pierrehumbert, 1982: Dynamics of weather regimes: Quasi-stationary waves and blocking. *Mon. Wea. Rev.*, **110,** 1105–1145.

——, and S. Yang, 1993: The role of transients in weather regimes and transitions. *J. Atmos. Sci.*, **50,** 1173–1180.

Shutts, G. J., 1983: The propagation of eddies in diffluent jetstreams: Eddy vorticity forcing of "blocking" flow fields. *Quart. J. Roy. Meteor. Soc.*, **109,** 737–761.

——, 1986: A case study of eddy forcing during an Atlantic blocking episode. *Advances in Geophysics,* Vol. 29, Academic Press, 135–162.

Simmons, A. J., J. M. Wallace, and G. R. Branstator, 1983: Barotropic wave propagation and instability, and atmospheric teleconnection patterns. *J. Atmos. Sci.*, **40,** 1363–1392.

Tribbia, J. J., 1984: Modons in spherical geometry. *Geophys. Astrophys. Fluid Dyn.*, **30,** 131–168.

Vautard, R., B. Legras, and M. Deque, 1988: On the source of midlatitude low-frequency variability. Part I: A statistical approach to persistence. *J. Atmos. Sci.*, **45,** 2811–2843.

Verkley, W. T. M., 1987: Stationary barotropic modons in westerly background flows. *J. Atmos. Sci.*, **44,** 2382–2398.

——, 1993: A numerical method for finding form-preserving free solutions of the barotropic vorticity equation on a sphere. *J. Atmos. Sci.*, **50,** 1488–1503.